AAPS PharmSciTech **2004; 5 (1) Article 18 (http://www.aapspharmscitech.org).**

Experimental Design for the Formulation and Optimization of Novel Cross-Linked Oilispheres Developed for In Vitro Site-Specific Release of *Mentha piperita* Oil

Submitted: November 5, 2003; Accepted: February 18, 2004

Wilbert Sibanda,[1] Viness Pillay,[2] Michael P Danckwerts,[1] Alvaro M Viljoen,[1] Sandy van Vuuren,[1] and Riaz A Khan[2]

[1]University of the Witwatersrand, Department of Pharmacy and Pharmacology, Medical School, Johannesburg 2193, South Africa

[2]Florida A&M University, College of Pharmacy and Pharmaceutical Sciences, Tallahassee, FL 32307

ABSTRACT

A Plackett-Burman design was employed to develop and optimize a novel crosslinked calcium-aluminum-alginate-pectinate oilisphere complex as a potential system for the in vitro site-specific release of *Mentha piperita*, an essential oil used for the treatment of irritable bowel syndrome. The physicochemical and textural properties (dependent variables) of this complex were found to be highly sensitive to changes in the concentration of the polymers (0%-1.5% wt/vol), crosslinkers (0%-4% wt/vol), and crosslinking reaction times (0.5-6 hours) (independent variables). Particle size analysis indicated both unimodal and bimodal populations with the highest frequency of 2 mm oilispheres. Oil encapsulation ranged from 6 to 35 mg/100 mg oilispheres. Gravimetric changes of the crosslinked matrix indicated significant ion sequestration and loss in an exponential manner, while matrix erosion followed Higuchi's cube root law. Among the various measured responses, the total fracture energy was the most suitable optimization objective (R^2 = 0.88, Durbin-Watson Index = 1.21%, Coefficient of Variation (CV) = 33.21%). The Lagrangian technique produced no significant differences ($P > .05$) between the experimental and predicted total fracture energy values (0.0150 vs 0.0107 J). Artificial Neural Networks, as an alternative predictive tool of the total fracture energy, was highly accurate (final mean square error of optimal network epoch ≈0.02). Fused-coated optimized oilispheres produced a 4-hour lag phase followed by zero-order kinetics (n > 0.99), whereby analysis of release data indicated that diffusion (Fickian constant k_1 = 0.74 vs relaxation constant k_2 = 0.02) was the predominant release mechanism.

Corresponding Author: Viness Pillay, Florida A&M University, College of Pharmacy and Pharmaceutical Sciences, Tallahassee, FL 32307; Tel: (850) 599-3511; Fax: (850) 599-3934; Email: viness.pillay@famu.edu

KEYWORDS: Plackett-Burman design, *Mentha piperita* oil, crosslinked oilisphere delivery system, constrained optimization, Artificial Neural Networks, lag-time with zero-order kinetics

INTRODUCTION

Irritable bowel syndrome (IBS), a functional disorder of the intestines, is characterized by severe abdominal cramps and constipation with alternating periods of diarrhea. Population-based studies in the United States estimate the prevalence of IBS at 10% to 20% and the incidence at 1% to 2% per year.[1] The primary cause of IBS appears to be related to altered intestinal motility patterns. Patients experience rigid contractions and pain in the bowel, which are responsible for the sensation of bloating, discomfort, and urgency, a symptom-complex thought to be regulated by the hypothesized "brain-gut-axis" relationship.[2,3] Over the years, many drug classes have been used for the alleviation of IBS symptoms, including antidiarrheals, antiflatulants, anticholinergics, opioids, low-dose antidepressants, and most recently serotonin antagonists.

In recent years, there has been a shift toward the use of natural products for IBS therapy. In this regard, multicenter clinical trials have already demonstrated positive outcomes in the treatment of patients, demonstrating significant alleviation of the symptoms associated with IBS through the use of *Mentha piperita* oil (commonly known as peppermint oil). This effect is related to the ability of peppermint oil to block the influx of calcium, thereby inhibiting abnormal smooth muscle contraction of the intestine.[4-6]

In general, the oil is rich in monoterpenes and sesquiterpenes. The principal components are the monoterpenes: menthol, menthone, and menthyl acetate.[7] Among these monoterpenes, menthol is the primary bioactive constituent. Pharmaceutical grade oil is standardized to contain no less than 44% free menthol.

Table 1. The Plackett-Burman Matrix Design

Oilisphere Formulation No.	Run Order	Sodium Alginate % wt/vol	Pectin % wt/vol	Calcium Chloride % wt/vol	Aluminum Chloride % wt/vol	Aluminum Sulfate % wt/vol	Crosslinking Reaction Time (hours)
F1	7	0	1.5	4	4	0	6
F2	11	1.5	0	4	0	0	0.5
F3	6	1.5	0	0	0	4	6
F4	12	0	1.5	0	0	0	6
F5	14	1.5	1.5	0	4	0	0.5
F6	2	1.5	1.5	0	4	4	0.5
F7	5	0	0	0	0	0	0.5
F8	9	1.5	0	4	4	0	6
F9	3	0	0	4	4	4	0.5
F10	13	0.75	0.75	2	2	2	3.25
F11	4	0.75	0.75	2	2	2	3.25
F12	8	0	0	0	4	4	6
F13	10	1.5	1.5	4	0	4	6
F14	1	0	1.5	4	0	4	0.5

Currently, the enteric-coated monolithic dosage form is the most widely used approach to achieve intestinal delivery of *Mentha piperita* oil.[8-11] Enteric delivery of this oil is essential for 2 reasons: (1) contact with the gastric mucosa results in muscle relaxation and hence severe esophageal reflux, and (2) the oil is hydrolyzed at gastric pH. One of the key problems with monolithic drug delivery systems is their unpredictable and erratic gastric emptying rates. In IBS patients, this rate is further altered by the hypothesized "brain-gut-axis" relationship.[12-14] Traditionally, erratic gastric emptying rates have more negatively influenced the effectiveness of enteric-coated dosage forms such as tablets and softgels, leading to variable absorption and pharmacologic response. Overall, we believe that these limitations may be circumvented through the application of multiple-unit technology. The choice of multiple units is based on their well-known advantages, such as predictable gastric transit times, less localized gastrointestinal disturbances, and the ensurance of site-specific drug delivery.

Hence, the objective of this study was to develop an optimized spherical multiple-unit calcium-aluminum-alginate-pectinate formulation for the in vitro site-specific release of peppermint oil (henceforth referred to as "oilispheres"). The pH conditions of the proximal and distal intestine were simulated using an in vitro 1-octanol buffer system. To achieve the objective of this study, a Plackett-Burman design was adopted. The application of this optimization technique provided an efficient and economical method to acquire the necessary information to understand the relationship between the controllable (independent) and performance (dependent) variables.[15-19] The independent variables that were evaluated included different levels of alginate and/or pectin exposed to varying reaction times in an aqueous calcium chloride/aluminum chloride/aluminum sulfate crosslinking solution. The responses measured from these reactions included matrix resilience, hardness, total fracture energy, erosion, and the pH-dependent in vitro release characteristics. Final formulation selection was achieved using a constrained optimization technique. In addition, we compared the predictive power of the Plackett-Burman regression model to that of a Generalized Feed Forward (GFF) Artificial Neural Network (ANN) algorithm.

MATERIALS AND METHODS

A low-viscosity sodium alginate (35cP for a 1% wt/vol aqueous solution at 21°C) was obtained from TIC Gums (Belcamp, MD). Low methoxyl citrus pectin (degree of esterification 34%-38%) was donated by Herbstreith and Fox (Neuenburg/Wurttemberg, Germany). Anhydrous calcium chloride, aluminum chloride, and aluminum sulfate were purchased from Sigma (St Louis, MO). Pharmaceutical grade *Mentha piperita* oil (composed of 67% menthol) was obtained from Aromatherapy Oils (Johannesburg, South Africa). Gas chromatography–grade menthol standard (≥99% purity) was purchased from Sigma. Spectrophotometric-grade 1-octanol was purchased from Fluka Chemicals (Buchs, Switzerland).

Developing the Experimental Design

In this study, the aim was to screen the overall main interactions effects among 6 independent variables (Table 1) in an economical manner. Under these circumstances (ie, when >5 factors are studied), the Plackett-Burman design is highly recommended.[20] Higher-order linear full factorial and quadratic Box-Behnken designs would have required 66 and 52

Table 2. Textural Parameters Employed for Total Fracture Energy, Matrix Hardness, and Resilience Testing

Parameters	Total Fracture Energy and Matrix Hardness Settings	Resilience Settings
Pretest speed	1 mm/s	1 mm/s
Test speed	0.2 mm/s	0.2 mm/s
Posttest speed	0.2 mm/s	0.2 mm/s
Compression force/distance	60 N	50% strain
Trigger type	Auto	Auto
Trigger force	0.5 g	0.5 g
Load cell	5 kg	5 kg

experimental runs, respectively, which was prohibitively uneconomical.

Matrices comprised either singly or in combination with alginate and/or pectin (0%-1.5% wt/vol) were crosslinked for different periods of time (0.5-6 hours) in calcium chloride, aluminum chloride, and/or aluminum sulfate (0%-4% wt/vol). Unhydrated matrix resilience (%), hydrated matrix resilience (%) in buffer media pH 3 and 6.8, matrix hardness (N/m), total fracture energy (Joules), and normalized matrix erosion in buffer media pH 3 and 6.8 were selected as the dependent variables (responses) in order to evaluate the physicochemical properties of the crosslinked matrices. Essential Regression and Experimental Design, Version 2.2 (Gibsonia, PA) was used to generate the statistical matrix, which required 14 experimental runs (12 model runs and 2 center points) (Table 1). The formulations were produced and tested in a random sequence.

The regression model (Equation 1) encompassing 7 linear terms was as follows:

$$\text{Response} = b_0 + b_1*[\text{SA}] + b_2*[\text{P}] + b_3*[\text{CC}] + b_4*[\text{AC}] + b_5*[\text{AS}] + b_6*\text{CRT} \quad (1)$$

where the terms represent the concentrations of polymers and crosslinking agents (in parentheses) as well as the crosslinking reaction time; $b_0 \ldots b_6$ are the regression coefficients of the system; SA indicates sodium alginate; P, pectin; CC, calcium chloride; AC, aluminum chloride; AS, aluminum sulfate; and CRT, crosslinking reaction time.

Formulation of Crosslinked Oilispheres

Oilispheres loaded with *Mentha piperita* oil were formulated in accordance with the Plackett-Burman design having polymer/crosslinking agent concentrations, crosslinking reaction times, and their combinations as depicted in Table 1.

A quantity of sodium alginate and/or pectin was dissolved in deionized water and made up to volume (100 mL). To this solution, 50 mL of *Mentha piperita* oil was added. Thereafter, this multicomponent solution was gently homogenized for 2 minutes to produce a polymer-oil emulsion (Homomixer, Chemineer, Inc, North Andover, MA). The crosslinking solution was prepared by dissolving an appropriate quantity of calcium chloride, aluminum chloride, and/or aluminum sulfate in deionized water and made up to volume (1000 mL). The polymer-oil emulsion was titrated at 2 mL/minute into the crosslinking solution using a 6-channel peristaltic pump (Desaga, Heidelberg, Germany) via PharMed tubing (Cole-Parmer, Vernon Hills, IL) fitted with a flat-tip, 19-gauge needle at the end. On completion of this titration, the formed oilispheres were agitated in the crosslinking solution for an additional 30 minutes. Thereafter, the oilispheres were allowed to equilibrate under dark conditions (±21°C) for a predetermined crosslinking reaction time (Table 1). Following this equilibration phase, the crosslinking solution was decanted, and the oilispheres were washed with 3 × 500-mL volumes of deionized water. The oilispheres were air dried at ±21°C for 48 hours under an extractor.

Physicomechanical Analysis of Crosslinked Oilispheres by Textural Profiling

To determine the resilience, total fracture energy, and matrix hardness of the oilispheres, a TA.XT.*plus* Texture Analyzer (Stable Micro Systems, Surrey, UK) fitted with a 36-mm cylindrical steel probe and 5-kg load cell was used. In order to determine the effect of hydration on the resilience of the oilispheres, a modified *United States Pharmacopeia (USP)* 25 rotating paddle method was used. In summary, the hydration media comprised an upper phase of 1-octanol (300 mL) and a lower phase of either hydrochloric acid buffer, pH 3, or phosphate buffer, pH 6.8 (600 mL). (Refer to Pillay and Fassihi[21] for more information on the rationale of this 2-phase solvent system.) At appropriate time intervals, oilispheres were removed from the lower phase (N = 10) and analyzed in accordance with the parameters listed in Table 2.

Figure 1A depicts the points used in the calculation of matrix resilience, which is provided by the ratio of the area under the curve (AUC) between anchors 2 and 3, and 1 and 2. Figure 1B indicates the calculation of the total fracture en-

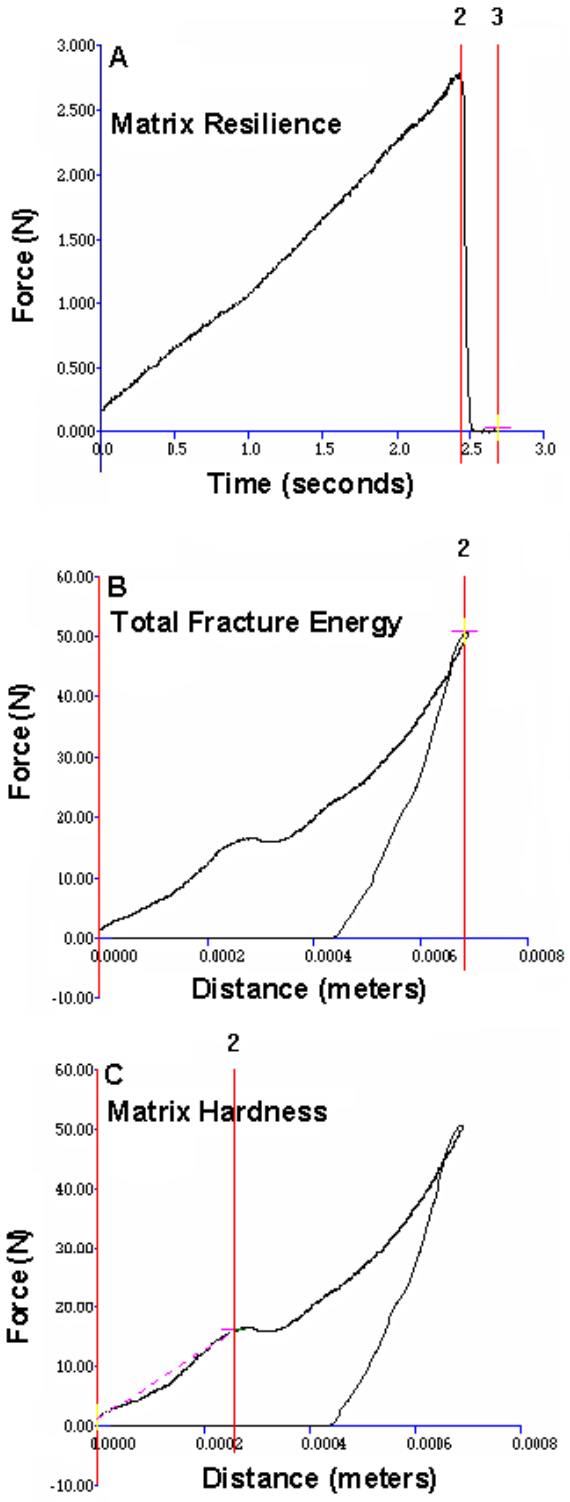

Figure 1. Typical force-time and force-distance profiles of crosslinked oilispheres employed in the calculation of key textural parameters. (In all cases it was observed that SDs < 0.03 were obtained, N = 10).

ergy, which is provided by the total AUC of a force-distance profile resembling the various phases of matrix fracture (ie, AUC between anchors 1 and 2). The first break in the upward gradient is indicative of a primary matrix facture, which results in a force reduction. However, on further application of the force, the residual intact matrix undergoes complete fracture, and hence the force peaks at 60 N. Figure 1C depicts the points used in the calculation of matrix hardness, which is indicated by the steepness of the upward gradient up to the primary fracture, namely, between anchors 1 and 2. In general, a steeper gradient indicates a harder matrix.

Oilisphere Size Analysis

The various oilisphere formulations were subjected to particle size analysis by employing a nest of 10 sieves ranging from 5000 to 150 mm agitated on a sieve shaker set at medium amplitude for 5 minutes (Octagon 200 Test Sieve Shaker, Endecotts Ltd, London, UK). The various size fractions were collected and stored separately in glass vials until further use.

Determination of Mentha piperita *Oil Encapsulation*

Fifty milligrams of oilispheres from each formulation was ground in a glass mortar to release the oil. To this pulverized mass, 300 mL 1-octanol and 600 mL phosphate buffer, pH 6.8, was added. The 1-octanol-phosphate buffer combination was magnetically stirred for 1 hour to facilitate complete diffusion (partitioning) of the oil into the 1-octanol phase. This 2-phase system was allowed to equilibrate for a further hour. Five-milliliter samples were withdrawn from the 1-octanol layer (N = 3) using a 0.45-µm Millipore filter (Millipore, Billerica, MA) attached to a glass syringe and analyzed for menthol content by UV spectroscopy at the wavelength maximum of 230 nm (Beckman DU 650 UV spectrophotometer, Beckman Coulter, Inc, Fullerton, CA) since menthol is the principal bioactive component of *Mentha piperita* oil.

It is well known that gas chromatography (GC) is the method of choice for the analysis of essential oils.[22-24] However, in this study it was found that menthol standard curves generated by GC and UV methods showed no significant differences ($y = 1.6988x + 0.03$, $R^2 = 0.98$, $P > .05$). UV was selected as the method of choice for analysis because of its ease of operation and time-saving capability. Note that GC required a 45-minute run per sample. Inter- and intraday precision (% Relative Standard Deviation [RSD%]) for menthol were well within ±2%, and accuracy within 98.2% to 101.3%. Repeatability and reproducibility were found to be excellent, within an RSD of <1%. The limit of detection and limit of quantitation in 1-octanol were 0.05 and 0.15 mg/mL, respectively.

In Vitro Release Studies

In vitro release studies (Caleva Dissolution Apparatus, model 7ST, G.B. Caleva Ltd, Dorset, UK) on a quantity of oilispheres equivalent to 50 mg of *Mentha piperita* oil (N = 3) were performed on optimized formulations using the above-mentioned modified *USP* 25 rotating paddle 2-phase solvent method (37°C, 50 rpm).[21] The lower phase consisted of 600 mL of *USP*-recommended buffers of either pH 1.5, 4.0, or 6.8, while the upper phase consisted of 300 mL of 1-octanol. The oilisphere samples were introduced into the buffer phase below a ring-mesh device prior to the addition of 1-octanol. Five-milliliter samples of 1-octanol were withdrawn through a 0.45-µm Millipore filter attached to a glass syringe at appropriate time intervals and analyzed by UV spectroscopy at 230 nm. An equivalent volume of oil-free 1-octanol was replaced into each vessel sampled.

Determination of Gravimetric Changes of the Oilisphere Matrix

Fifty milligrams of oilispheres were accurately massed (N = 3) and placed into dissolution vessels containing 600 mL of buffer of either pH 3 or pH 6.8 maintained at 37°C with paddles operated at 50 rpm. At appropriate time intervals, the entire quantity of remaining oilispheres was removed from the buffer medium and dried to constant weight at ±21°C under an extractor. The mass of the dried residue was normalized to express the erosion of the matrix.

Microwell Plate Coating of Oilispheres

A novel fusion coating procedure was developed to attach oil-free crosslinked and uncrosslinked peripheral polymeric layers around the oilispheres. Individual oilispheres were introduced into microwells having a 200-µL capacity. In the first case, a 2% wt/vol binary coating solution of a 1:1 combination of alginate and pectin was prepared (viscosity of 920 cP at 21°C), of which 50 µL was added to each microwell containing an oilisphere. The plate was thereafter agitated for 30 seconds on a vortex (Genie Vortex-2, Scientific Industries, Bohemia, NY) to ensure that the oilispheres were completely coated with the binary mixture. This procedure provided an uncrosslinked peripheral layer around the oilispheres. In the second case, the same procedure was applied, except for the addition of 50 µL of a crosslinking agent consisting of an aqueous solution of 4% wt/vol each of calcium chloride, aluminum chloride, and aluminum sulfate to induce fusion between the crosslinked peripheral polymer and the surface of the oilisphere. Both sets of oilispheres comprising the uncrosslinked and crosslinked peripheral layers were dried at ±21°C for 48 hours under an extractor.

RESULTS AND DISCUSSION

Sieve Analysis

Typically unimodal and bimodal size distributions were observed, showing the 2-mm oilispheres as having the highest frequency (Figure 2). This size fraction was chosen for all investigations in this study. Bimodal distribution was attributed to deaggregation of the homogenized droplets into smaller and larger populations during the crosslinking process as a result of a high interfacial tension that would be expected between the surface of the aqueous crosslinking solution and the oily residue around the periphery of the droplets. This oily residue may have prevented rapid interaction between the polymer and crosslinking solution, hence leading to heterogeneous separation of a single droplet.

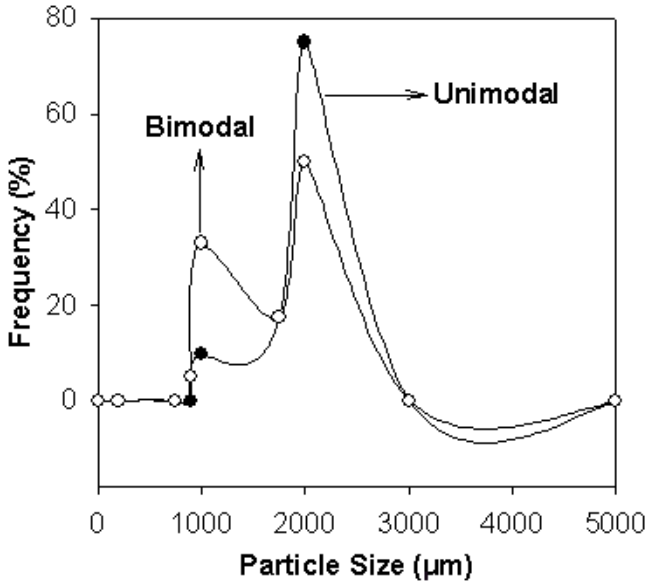

Figure 2. Size distribution of the crosslinked oilisphere matrices indicating unimodal and bimodal profiles. (In all cases it was observed that SDs < 0.06 were obtained, N = 3).

Oil Encapsulation

Encapsulation of *Mentha piperita* oil ranged between 6 and 35 mg per 100-mg oilispheres (Figure 3). This range was attributed to the large differences in the degree of crosslinking and hence the significant variation in the encapsulation efficiency. Oilispheres with a low crosslink density demonstrated low encapsulation. A relationship between specific textural parameters and the degree of crosslinking has already been established by Pillay and coworkers.[25,26]

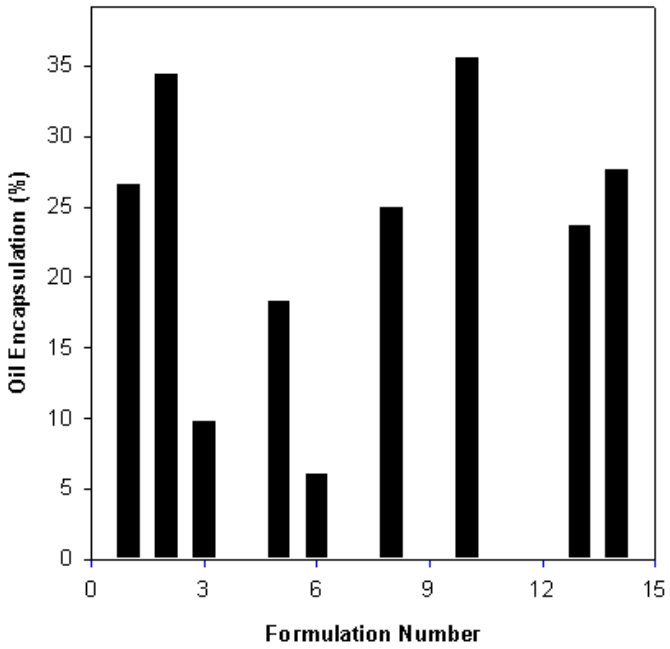

Figure 3. Encapsulation efficiency of *Mentha piperita* oil within the crosslinked matrices. (In all cases it was observed that SDs < 0.1 were obtained, N = 3).

Gravimetric Transitions of the Crosslinked Matrix

It should be noted that matrix erosion can have an effect on the release of drugs and other bioactive substances from their delivery systems. In this study, essentially 2 types of weight change behavior were noted upon hydration of the oilispheres in either phosphate buffer pH 3 or pH 6.8 (Figures 4A and B).

In the first instance, there was an increase in the oilisphere weight during the first 2 hours of hydration. This increase was attributed to the sequestration of phosphate ions from the release medium, which was thereafter followed by a plateau (Figure 4A). The ionic threshold concentration for sequestration has previously been mathematically described by Pillay and Fassihi.[25] Curve-fitting of these data (Figure 4A) indicated that such behavior followed an exponential rise to a maximum ($R^2 > 0.99$), as described by the following equation:

$$M_t = M_0\left(1 - e^{-k_{seq}t}\right) \qquad (2)$$

where M_t indicates the mass of matrix at time t; M_0, original mass of matrix; and k_{seq}, exponential rate constant of ion sequestration.

In the second instance (Figure 4B), 3 phases were observed. Initially, there was a rapid decline in the matrix weight (phase 1), followed by ion sequestration (phase 2), and then rapid erosion to a plateau (phase 3), indicating complete matrix dissolution. Curve-fitting of these data indicated that these phases could be described by the following equations, each producing an $R^2 > 0.99$.

Phase 1 - Simple exponential loss of soluble ions from the surface of the oilisphere:

$$M_t = M_0\, e^{-k_{sol}t} \qquad (3)$$

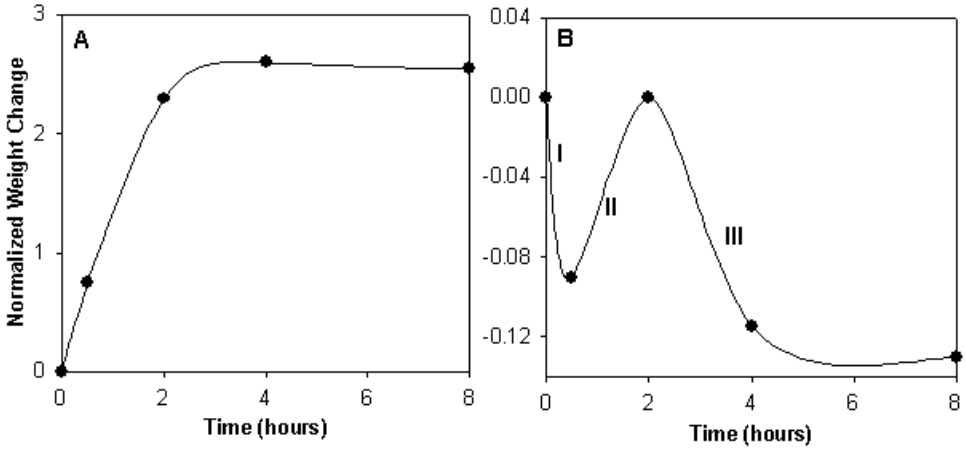

Figure 4. Erosional behavior of the crosslinked oilispheres depicting (A) ion sequestration and (B) 3 phases of ion loss, sequestration, and matrix erosion. (In all cases it was observed that SDs < 0.1 were obtained, N = 3).

where k_{sol} is the first-order solubility constant rate of the ions.

Phase 2 - As the oilisphere starts to swell, it exponentially sequesters these ions back into the matrix:

$$M_t = M_0 e^{k_{seq}t} \quad (4)$$

where k_{seq} is the exponential rate constant of ion sequestration.

Phase 3 - Higuchi-type erosion of the matrix represented by the cube root of time equation:

$$M_t = k_{ero} \sqrt[3]{t} \quad (5)$$

where k_{ero} is the matrix erosion rate constant.

Physicomechanical Behavior of Crosslinked Oilispheres

Textural profiling revealed a decrease in the total fracture energy, and an increase in matrix hardness and resilience, in relation to the statistical combinations and concentrations of the crosslinkers. In general, aluminum chloride and sulfate provided matrix reinforcement, while calcium chloride principally crosslinked the polymeric system, as determined from preformulation work. Hence, these ions were selected as the ionotropic agents in this study.

Macros run on Texture Exponent Version 3.2 (Stable Micro Systems, Surrey, UK) were able to simultaneously calculate the values for matrix resilience (unhydrated and hydrated), matrix hardness, and total fracture energy (Table 3). Table 3 also clearly outlines that all oilisphere formulations had very low total fracture energy values, indicating that the matrix was fragile and hence collapsed upon application of a 60N force.

Stepwise Regression Analysis

Using Essential Regression and Experimental Design, repeated forward and backward stepwise regression was employed to generate the equations for each response parameter, which essentially is represented by Equation 1, since all independent variables were statistically fitted to show both the significant and insignificant terms. The predicted and experimental values for each response parameter shown in Table 3 were correlated by the Cook's Distance (CD), which provides a measurement of the overall influence of each observation on the regression coefficients, including the intercept. The CD values presented in Table 3 are rounded off to 2 decimal places for convenience. The complete values up to 6 decimal places were used for correlation purposes. Figures 5 and 6 depict the close correlation between the experimental and predicted data obtained for each of the responses in relation to the formulations outlined in the Plackett-Burman design ($P > .05$). However, based on the large variation in the experimental response values for each formulation (F1-F14) it is evident that different degrees of crosslinking are manifested by significant changes in the physicomechanical properties of the oilisphere matrix.

Constrained Optimization

Among different techniques that are available for solving constrained optimization problems, the most common are the Lagrangian and Simplex methods. In this study, optimization was accomplished by the Lagrangian approach originally introduced by Fonner and coworkers,[27] using the Solver function of Microsoft Excel 2002.[16]

Tables 4 and 5 provide a detailed analysis of the mathematical fit of data for each response function and their levels of significance. Such analysis is required for the final selection of the objective function to be applied in the constrained optimization.

Regression on the unhydrated matrix resilience and hardness produced suitable R^2 values, while on the other hand significantly high CV values were obtained. The total fracture energy comparatively produced statistically desirable values (high R^2, low CV), also indicating that the model was 88% accurate with regards to data prediction by regression. Hence, it was selected as the optimization objective.

The following constraints (percentage wt/vol concentration, hours) were imposed on the independent variables, using the work of Pillay and Danckwerts[26] as a novel reference point to generate an ideal in vitro release profile for *Mentha piperita* oil:

- $1 \leq$ [sodium alginate] ≤ 2
- $1 \leq$ [pectin] ≤ 2
- $1 \leq$ [calcium chloride] ≤ 6
- $1 \leq$ [aluminum chloride] ≤ 6
- $1 \leq$ [aluminum sulfate] ≤ 6
- $0.5 \leq$ crosslinking reaction time (hours) ≤ 6

The lower limit of 1% wt/vol for both polymers and crosslinking agents was the necessary minima for the production of spherical oilispheres. The concentration of sodium alginate and pectin beyond 2% wt/vol was not feasible since accurate titration was significantly inhibited by their excessively high viscosity. The upper limit of 6% wt/vol for the crosslinking agents was based on the ability to produce optimal crosslinking. The crosslinking reaction times were

Table 3. Correlation Between Predicted and Experimental Responses Generated From the Plackett-Burman Design*

Oilisphere Formulation	Unhydrated Matrix Resilience			Hydrated Matrix Resilience pH 3			Hydrated Matrix Resilience pH 6.8			Matrix Hardness			Total Fracture Energy			Normalized† Matrix Erosion pH 3			Normalized Matrix Erosion pH 6.8		
	Exp (%)	Pred (%)	CD	Exp (%)	Pred (%)	CD	Exp (%)	Pred (%)	CD	Exp (N/m)	Pred (N/m)	CD	Exp (J)	Pred (J)	CD	Exp	Pred	CD	Exp	Pred	CD
F1	8.48	27.92	0.32	3.98	11.18	0.08	3.22	5.28	0.10	6341.82	-674.55	0.22	0.010	0.007	0.04	0.301	0.141	0.03	0.561	-1.131	0.03
F2	3.08	38.11	0.46	4.27	19.35	0.36	0.63	4.96	0.46	4142.10	-329.75	0.09	0.014	0.011	0.02	0.003	-0.008	0.06	-0.186	-0.208	0.01
F3	7.97	38.11	0.32	23.93	35.10	0.20	4.25	4.21	2.87	5433.84	6142.50	0.02	0.012	0.011	0.12	2.341	2.031	0.02	4.264	1.932	0.02
F4	0	27.92	0.13	0	10.08	0.16	0	0.97	0.08	0	-1504.70	0.01	0.009	0.007	0.02	0	0.308	0.03	0	0.384	0.03
F5	102.01	77.68	0.14	4.47	2.279	0.00	1.56	3.91	0.02	15571.76	30530.60	1.03	0.014	0.017	0.00	1.724	1.508	0.04	-0.035	-0.768	0.01
F6	71.02	77.68	0.32	4.23	13.07	0.12	3.75	2.92	0.13	54411.6	37846.40	0.10	0.016	0.017	0.00	0.012	0.099	0.02	-0.726	-0.299	0.04
F7	0	-11.65	0.25	0	-12.41	0.25	0	-0.73	0.01	0	-4859.60	0.01	0.003	0.001	0.02	0	0.007	0.05	0	0.357	0.02
F8	47.64	38.11	0.03	23.23	25.41	0.03	13.93	9.51	0.01	1582.42	-343.20	0.04	0.009	0.011	0.22	-0.531	-0.252	0.01	-0.841	-0.051	0.03
F9	0	-11.65	0.06	0	-0.522	0.06	0	2.58	0.48	0	3286.40	0.04	0.003	0.001	0.02	0	-0.001	0.01	0	-0.690	0.03
F10	53.72	33.02	0.04	34.64	14.71	0.01	8.04	3.49	0.16	2641.74	7461	0.05	0.011	0.009	0.00	-0.330	-0.022	0.02	-0.916	-0.002	0.02
F11	53.72	33.02	0.02	34.64	14.71	0.01	8.04	3.49	0.01	2641.74	7461	0.02	0.011	0.009	0.00	-0.330	-0.412	0.02	-0.916	-0.002	0.08
F12	0	-11.65	0.01	0	4.439	0.03	0	2.83	0.01	0	2442.80	0.02	0.002	0.001	0.03	0	0.001	0.05	0	0.981	0.02
F13	94.95	77.68	0.49	67.76	52.63	0.37	2.51	5.67	0.19	7864.98	10341	0.03	0.018	0.017	0.09	-0.475	0.481	0.02	-0.665	0.288	0.04
F14	19.65	27.92	0.01	4.77	15.91	0.20	2.89	-0.26	0.24	3822.48	6654.70	0.07	0.011	0.007	0.03	-0.538	-0.478	0.01	-0.563	-0.818	0.03

*Exp indicates experimental value for response; Pred, predicted value for response; and CD, Cook's Distance.

†Values are normalized such that the reference point is zero.

Table 4. Regression Diagnostics for Completely Fitted Responses*

Responses Measured	R^2	Durbin-Watson Index (%)	CV (%)
Unhydrated Matrix Resilience (%)	0.74	1.45	77.26
Hydrated Matrix Resilience: pH 3 (%)	0.63	1.60	112.42
Hydrated Matrix Resilience: pH 6.8 (%)	0.41	1.94	121.74
Matrix Hardness (N/m)	0.74	2.20	131.60
Total Fracture Energy (J)	0.88	1.75	33.21
Gravimetric Transitions: pH 3	0.42	1.21	79211.24
Gravimetric Transitions: pH 6.8	0.37	1.75	78918.52

*CV indicates Coefficient of Variation.

Table 5. Level of Significance of Regression Coefficients Generated in the Linear Model of Each Response Parameter at a 95% Confidence Interval ($P < .05$)*

Coefficient	Independent Variables	UMR (%)	HMR: pH 3 (%)	HMR: pH 6.8 (%)	MH (N/m)	TFE (J)	GT: pH 3	GT: pH 6.8
b0	-	0.376	0.314	0.780	0.616	0.804	0.832	0.804
b1	[SA]	0.01178	0.07611	0.206	0.05355	0.00061	0.431	0.722
b2	[P]	0.03123	0.574	0.751	0.05837	0.01127	0.546	0.373
b3	[CC]	0.937	0.253	0.385	0.173	0.08114	0.435	0.324
b4	[AC]	0.280	0.295	0.434	0.140	0.598	0.423	0.453
b5	[AS]	0.725	0.296	0.698	0.238	0.367	0.654	0.584
b6	CRT	0.690	0.121	0.339	0.139	0.620	0.323	0.357

*UMR indicates unhydrated matrix resilience; HMR, hydrated matrix resilience; MH, matrix hardness; TFE, total fracture energy; GT, gravimetric transition; SA, sodium alginate; P, pectin; CC, calcium chloride; AC, aluminum chloride; AS, aluminum sulfate; and CRT, crosslinking reaction time.

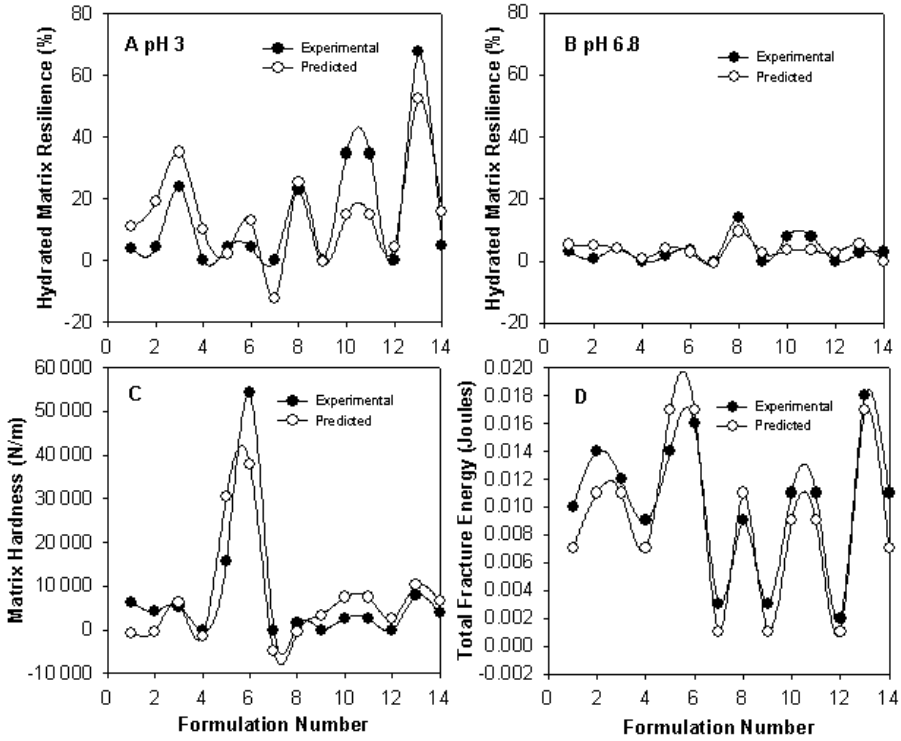

Figure 5. Correlation between experimental data and values predicted by the response models for (A) hydrated matrix resilience in buffer medium pH 3, (B) hydrated matrix resilience in buffer medium pH 6.8, (C) matrix hardness, and (D) total fracture energy. Note that the unhydrated matrix resilience (not shown) was overall ≈20% higher than that of the hydrated matrices. (In all cases for the experimental studies it was observed that SDs < 0.02 were obtained, N = 10).

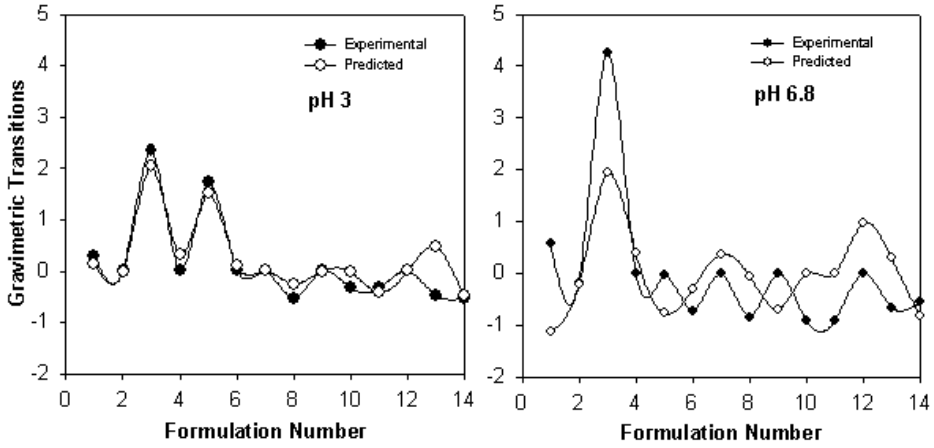

Figure 6. Correlation between experimental data and values predicted by the response model for gravimetric transitions in buffer media of pH 3 and pH 6.8. (In all cases for the experimental studies SDs < 0.05 were obtained, N = 10).

Table 6. Composition of the Optimized Oilisphere Formulation Obtained by the Constrained Optimization Technique and Comparison of Experimental and Predicted Total Fracture Energy Values

Formulation Components	**Concentrations (% wt/vol) and Reaction Time (hours)**
Sodium alginate	1.5
Pectin	1.5
Calcium chloride	4
Aluminum chloride	4
Aluminum sulfate	4
Crosslinking reaction time	3
Optimized Formulation Analysis	**Total Fracture Energy (Joules)**
Experimental	0.0115 ± 0.003 (N = 10)
Predicted	0.0107

based on minimization of the loss of *Mentha piperita* oil into the crosslinking solution.

Table 6 reflects the results based on the above constrained optimization for development of the ideal oilisphere formulation. The experimentally generated values for the total fracture energy were compared with those predicted in order to validate the accuracy of the model. Excellent correlation was obtained (Table 6).

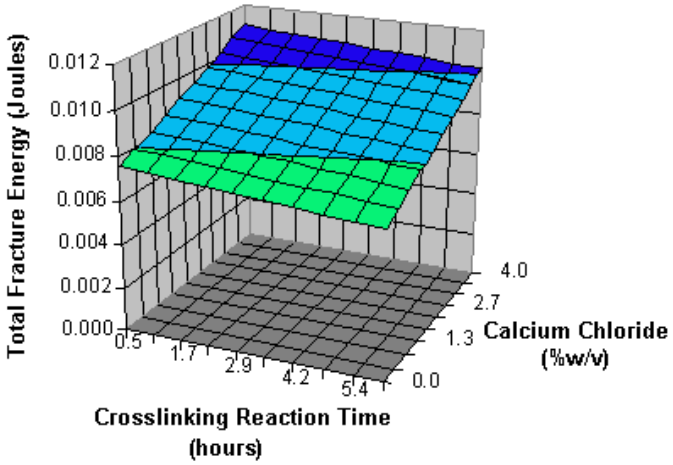

Figure 7. A typical surface response plot indicating the influence of increasing a crosslinker concentration and CRT on the total matrix fracture energy. Note that a similar effect was observed for the other crosslinkers (matrix reinforcers). An increase in the polymer concentration also increased the total fracture energy in a similar manner.

Figure 7 illustrates a typical surface response plot depicting the effects of the crosslinking reaction time and crosslinker concentrations on the total fracture energy. Note that all other combinations of the surface plots were analyzed but are not shown since those responses were statistically unstable. It was observed that as the concentration of calcium chloride was increased, the total fracture energy significantly increased. A similar effect was observed for aluminum chloride and aluminum sulfate. In order to achieve optimal matrix crosslinking, a maximum of 3 hours was required, without any significant effect beyond this time period. An increase in the polymer concentration also produced an increase in the total fracture energy.

Comparison of Predicted Response Values for Total Matrix Fracture Energy Using Artificial Neural Networks and the Plackett-Burman Regression Analysis

The application of ANN in advanced formulation design and development is being increasingly employed.[28-30] In this study, a GFF model was selected to predict the total fracture energy values using data generated from the Plackett-Burman design (see Tables 1 and 3). Essentially, a GFF is a generalization of a Multilayer Perceptron (MLP) such that network connections can jump over one or more hidden layers. In theory, an MLP can solve any problem that a GFF network can solve. In practice, however, GFF networks often solve the problem much more efficiently.[31,32] Such a network containing the same number of processing elements as a standard MLP requires less training, hence increasing the efficiency of neurocomputing.

For the hidden and output layers, a genetic algorithm with the SigmoidAxon transfer function and ConjugateGradient learning rule was employed respectively. A maximum of 5000 epochs were run 50 times on NeuroSolutions Version 4.24 (NeuroDimension Inc, Gainesville, FL) to ensure optimal training of data. Figure 8 illustrates the gradual leveling of the average mean square error (MSE) with standard deviation boundaries for the 50 runs, indicating the sequential improvement of model predictability. Table 7 reflects the average of the MSE values for all training runs, the best network run out of 5000 epochs repeated 50 times, and the efficiency of the GFF model in the training process. Overall, it is evident that the training model employed was highly efficient. The parameters depicted in Table 7 are standard statistical indicators used by scientists involved in neurocomputing to quantitate the accuracy of model prediction

Table 7. Neural Network Indicators Characterizing the Efficiency of Data Training*

Averages of the Minimum Training Errors	**Training Minimum**	**Training Standard Deviation**
Average of minimum MSEs	0.039647207	0.011162308
Average of final MSEs	0.039647207	0.011162308
Optimal Network Run Obtained From Data Training	**For Total Matrix Fracture Energy**	
Run no.	17	
Epoch no.	5000	
Minimum MSE	0.019716412	
Final MSE	0.019716412	
Performance of Neural Network by Testing of Training Data	**For Total Matrix Fracture Energy**	
MSE	1.57731E-05	
Normalized MSE	0.419817367	
Mean Absolute Error	0.002779493	
Minimum Absolute Error	5.16934E-06	
Maximum Absolute Error	0.009048942	
Correlation Coefficient	0.76189204	

*MSE indicates mean square error.

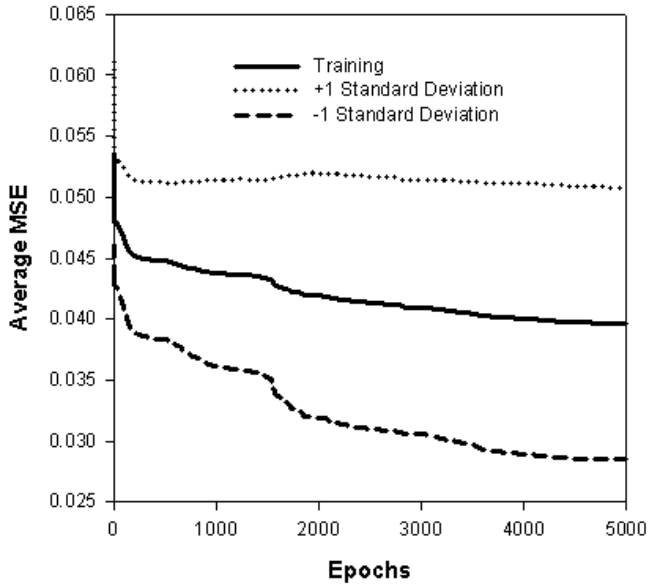

Figure 8. Average MSE with SD boundaries for 5000 epochs repeated 50 times.

and to subsequently select the optimal model (eg, MLP vs GFF algorithm).

Using all 14 formulations, the total matrix fracture energy was predicted by both the Plackett-Burman design and GFF neural model. The mean differences between the experimental and predicted values for the total fracture energy obtained from the Plackett-Burman design and neural model showed no significant differences (P = 0.265), using a 2-tailed paired Student t test. However, as a predictive tool, ANN appears to be a better choice, since as a data modeling process, it is easy, saves time, and does not require any critical need to mathematically factor out solutions. On the other hand, the Plackett-Burman approach, like all other traditional experimental designs requires the researcher to possess strong mathematical modeling skills, is time consuming, and requires multiple independent variables. Traditional statistical analysis does not provide "ideal values" but rather yields a list of solutions ranging from the most to least significant. Alternatively, an ANN provides a solution that zooms in only on the target values.

Optimized In Vitro Site-Specific Release of Mentha piperita Oil Based on the Constrained Optimization Solution in Conjunction with Fusion Coating

Based on the fact that *Mentha piperita* oil is unstable in an acidic environment, its release must be prevented in the gastric region and targeted to the proximal and distal intestine.

Optimization studies using the total matrix fracture energy enabled the formulation of a pH-dependent zero-order releasing oilisphere system (Figure 9). Figures 9A, C, and E indicate the release of the oil in different buffer media, while Figures 9B, D, and F reflect a composite profile in sequentially changing media, simulating the gastrointestinal pH conditions.

Figure 9A indicates that at least 80% of *Mentha piperita* oil is released in pH 1.5 and pH 4.0. From the composite profile (Figure 9B) at least 20% of the oil is released in pH 1.5 and pH 4.0. In an attempt to resolve this apparent contradiction, a coat of alginate and pectin was applied by 2 approaches to individual oilispheres using a microwell plate (see Methods Section for details). Using the first approach without crosslinkers, coating of the oilispheres resulted in a decrease in drug release over the simulated physiological pH range of

1.5 to 6.8; however, release of the oil was still detected in the acidic medium (Figures 9C and D). Using the second approach with crosslinkers, coating of the oilispheres resulted in a 2- to 4-hour lag phase in the acidic environment prior to release of the oil in phosphate buffer pH 6.8 (Figures 9E and F). From a biopharmaceutical perspective, this lag phase provides adequate time for gastric emptying of multiple units to occur.[33] In light of the objectives of our study, this formulation was chosen as the ideal for purposes of site-specific delivery of *Mentha piperita* oil.

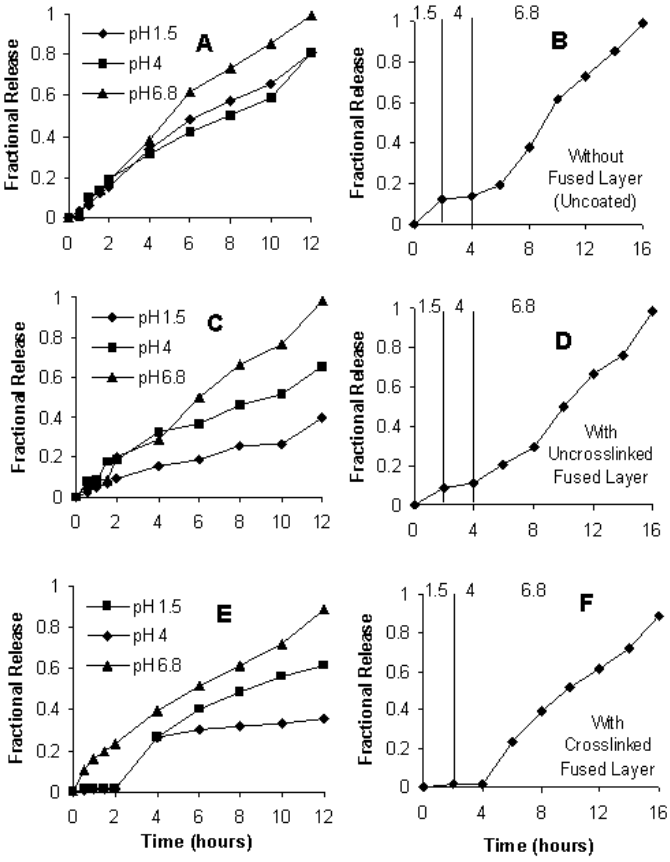

Figure 9. Release profiles of *Mentha piperita* oil from oilispheres in simulated gastric and intestinal fluid (pH 1.5, 4, 6.8): (A, B) without any coating; (C, D) with uncrosslinked fused coating; and (E, F) with crosslinked fused coating. (In all of the above cases SDs < 0.09 were obtained, N = 3).

Kinetic Modeling of Release Data From the Optimal Formulation

Various kinetic models were employed to identify the mechanism of release from the optimized oilispheres using data derived from the composite profile (Figure 9F), which essentially displayed site-specific biphasic release kinetics, characterized by a 4-hour lag phase prior to zero-order release. All least squares analysis used to determine the release mechanism of *Mentha piperita* oil was performed on WinNonlin Version 4.1 (Pharsight, Mountain View, CA) using the Gaussian-Newton (Levenberg-Hartely) approach.

The authors will not describe the equations below in detail as this information can be found elsewhere.[25] Kinetic modeling was applied using a modified form of the Power Law equation:

$$\frac{M_t}{M_\infty} = k_1 (t - t_L)^n \qquad (6)$$

where in the present study M_t is the amount of oil released at time t, M_∞ is the total amount of oil encapsulated within the oilispheres, k_1 is the Fickian kinetic constant, t_L represents the 4-hour lag time prior to release of the oil, and n is a release exponent.

Alternatively, Fickian diffusion and matrix relaxation/dissolution were analyzed using an expanded version of the Power Law equation:

$$\frac{M_t}{M_\infty} = k_1 (t - t_L)^n + k_2 (t - t_L)^{2n} \qquad (7)$$

where in this case k_2 is the relaxation/dissolution rate constant.

Hopfenberg's proposed model is either applicable to a slab, cylinder, or sphere showing heterogeneous erosion.[34] In order to account for the lag time, a modification to the original equation was made:

$$\frac{M_t}{M_\infty} = 1 - [1 - k_1 (t - t_L)]^n \qquad (8)$$

where in this case k_1 is the erosion rate constant, and n = 1, 2, and 3 for a slab, cylinder, and sphere, respectively.

Table 8 indicates the results from kinetic modeling of data up to 80% release.

At first glance, the values in Table 8 suggest that all 3 models suitably fit the release data based on the Akaike information criteria (AIC) and Schwartz criteria (SC) parameters. However, upon closer consideration of the condition number (CN) values, it is evident that the Hopfenberg model (Equation 8) is highly unstable (high value). The Power Law and its expanded variant (Equations 6 and 7) appear to suitably fit the data and statistically satisfy all parameters. Based on the n values and the low k_2 value in Equations 6 and 7, respectively, it is evident that diffusion is the predominant release mechanism. This finding is also clear considering that the oilisphere consists of a crosslinked peripheral coating, encapsulating the oil, and hence acts as a barrier to diffusion. Following the lag time of 4 hours, n and R^2

Table 8. Release Kinetics Obtained From the Various Diffusion, Relaxation, and Erosion Models*

Model M_t/M_∞=	k_1	k_2	n	AIC	SC	CN
$k_1(t-t_L)^n$ (Equation 6)	0.74	-	0.59	−48.49	−50.29	20.44
$k_1t^n + k_2t^{2n}$ (Equation 7)	0.13	0.02	0.56	−48.02	−50.72	21.26
$1-[1-k_1(t-t_L)]^n$ (Equation 8)	0.04	-	3	−42.25	−43.16	2377

*AIC indicates Akaike information criteria; SC, Schwartz criteria; CN, Condition number; M_t/M_∞, dependent variable; and t, independent variable.

values greater than 0.99 are achieved, indicating ideal zero-order kinetics.

CONCLUSION

Application of the Plackett-Burman design assisted in the successful formulation and optimization of a spherical crosslinked calcium-aluminum-alginate-pectinate oilisphere system for the in vitro site-specific release of *Mentha piperita* oil. The measured total fracture energy response was in close agreement with the predicted values of the optimized formulation, thereby demonstrating the feasibility of the optimization procedure in developing the crosslinked matrix. Kinetic modeling of data indicated that diffusion was the predominant release mechanism. Diffusion was modulated through the application of a novel fusion coating procedure. ANN, as an alternative tool to predict the response values of the dependent variables, is a very attractive approach when employing statistical strategies for formulation development.

ACKNOWLEDGEMENTS

Wilbert Sibanda acknowledges the grant (NRF 4467) for Novel Research from Adcock Ingram and the Graduate Research Fellowship from the National Research Foundation of South Africa.

REFERENCES

1. Madden JA, Hunter JO. A review of the role of the gut microflora in irritable bowel syndrome and the effects of probiotics. *Br J Nutr*. 2002;88(suppl):S67-72.

2. Allescher HD. Further extension of the brain-gut axis? *Neurogastroentero. Motil*. 2003;15:243.

3. Dunn AJ, Ando T, Brown RF, Berg RD. HPA axis activation and neurochemical responses to bacterial translocation from the gastrointestinal tract. *Ann N Y Acad Sci*. 2003;992:21-29.

4. Hills JM, Aaronson PI. The mechanism of action of peppermint oil on gastrointestinal smooth muscle. An analysis using patch clamp electrophysiology and isolated tissue pharmacology in rabbit and guinea pig. *Gastroenterology*. 1991;101:55-65.

5. Beesley A, Hardcastle J, Hardcastle PT, Taylor CJ. Influence of peppermint oil on absorptive and secretory processes in rat small intestine. *Gut*. 1996;39:214-219.

6. Zar S, Benson MJ, Kumar D. Review article: Bloating in functional bowel disorders. *Ailment Pharmacol Ther*. 2002;16:1867-1876.

7. Fleming T. *PDR for Herbal Medicines*. Montvale, NJ: Medical Economics Company Inc; 1998.

8. Liu JH, Chen GH, Yeh HZ, Huang CK, Poon SK. Enteric-coated peppermint oil capsules in the treatment of irritable bowel syndrome: prospective, randomized trial. *J Gastroenterol*. 1997;32:765-768.

9. Kline RM, Kline JJ, Di Palma J, Barbero GJ. Enteric-coated, pH-dependent peppermint oil capsules for the treatment of irritable bowel syndrome in children. *J Pediatr*. 2001;138:125-128.

10. Micklefield G, Jung O, Greving I, May B. Effects of intraduodenal application of peppermint oil (WS(R)1340) and caraway oil (WS(R)1520) on gastroduodenal motility in healthy volunteers. *Phytother Res*. 2003;17:135-140.

11. Weydert JA, Ball TM, Davis MF. Systemic review of treatments for recurrent abdominal pain. *Pediatrics*. 2003;111:e1-11.

12. Rosemore JG, Lacy BE. Irritable bowel syndrome: Basis of clinical management strategies. *J Clin Gastroenterol*. 2002;35(suppl 1):S37-S44.

13. Wood JD. Neuropathophysiology of irritable bowel syndrome. *J Clin Gastroenterol*. 2002;35(suppl 1):S11-S22.

14. Nakai A, Kumakura Y, Boivin M, et al. Sex differences of brain serotonin synthesis in patients with irritable bowel syndrome using alpha-[11C]methyl-L-tryptophan, positron emission tomography and statistical parametric mapping. *Can J Gastroenterol*. 2003;17:191-196.

15. Bonferoni MC, Rossi S, Ferrari F, Stavik E, Pena-Romero A, Caramella C. Factorial analysis of the influence of dissolution medium on drug release from carrageenan-diltiazem complexes. *AAPS PharmSciTech*. 2000;1(2):Article 15. Available at: http://www.aapspharmscitech.org.

16. Furlanetto S, Maestrelli F, Orlandini S, Pinzauti S, Mura P. Optimization of dissolution test precision for a ketoprofen extended-release product. *J Pharm Biomed Anal*. 2003;32:159-165.

17. Nazzal S, Khan MA. Response surface methodology for the optimization of ubiquinone self-nanoemulsified drug delivery system. *AAPS PharmSciTech*. 2002;3(1):Article 3. Available at: http://www.aapspharmscitech.org.

18. Prinn KB, Costantino HR, Tracy M. Statistical modeling of protein spray drying at the lab scale. *AAPS PharmSciTech*. 2002;3(1):Article 4. Available at: http://www.aapspharmscitech.org.

19. Prakobvaitayakit M, Nimmannit U. Optimization of polylactic-co-glycolic acid nanoparticles containing itraconazole using 23 factorial design. *AAPS PharmSciTech*. 2003;4(4):Article 71. Available at: http://www.aapspharmscitech.org.

20. NIST and SEMATECH. e-Handbook of Statistical Methods. Available at: http://www.itl.nist.gov/div898/handbook/. 2003.

21. Pillay V, Fassihi R. Evaluation and comparison of dissolution data derived from different modified release dosage forms: An alternative method. *J Control Release*. 1998;55:45-55.

22. Viljoen AM, Demarne FE, Van der Walt JJ. A study of the variation in the essential oil and morphology of *Pelargonium capitatum* (L) L'Herit.

(Geraniaceae). Part 2. The chemotypes of *P. Capitatum*. *J. Essent. Oil Res*. 1995;7:605-611.

23. Bruni R, Medici A, Andreotti E, et al. Chemical composition and biological activities of Ishpingo essential oil, a traditional Ecuadorian spice from *Ocotea quixos* (Lam.) Kosterm. (Lauraceae flower calices*Food Chem* 2004;85:415-421.

24. Howes M-JR, Simmonds MSJ, Kite GC. Evaluation of the quality of sandalwood essential oils by gas chromatography-mass spectrometry. *J Chromatogr A*. 2004;1028:307-312.

25. Pillay V, Fassihi R. In vitro release modulation from cross-linked pellets for site-specific drug delivery to the gastrointestinal tract. I. Comparison of pH-responsive drug release and associated kinetics. *J Control Release*. 1999;59:229-242

26. Pillay V, Danckwerts MP. Textural profiling and statistical optimization of cross-linked calcium-alginate-pectinate-cellulose acetophthalate gelisphere matrices. *J Pharm Sci*. 2002;91:2559-2570.

27. Fonner DE, Buck JR, Banker GS. Mathematical optimization techniques in drug product design and process analysis. *J Pharm Sci*. 1970;59:587-1596.

28. Ibric S, Jovanovic M, Djuric Z, et al. Artificial neural networks in the modeling and optimization of aspirin extended release tablets with Eudragit L 100 as matrix substance. *AAPS PharmSciTech*. 2003;4(1):Article 9. Available at: http://www.aapspharmscitech.org.

29. Leane MM, Cumming I, Corrigan OI. The use of artificial neural networks for the selection of the most appropriate formulation and processing variables in order to predict the in vitro dissolution of sustained release minitablets. *AAPS PharmSciTech*. 2003;4(2):Article 26. Available at: http://www.aapspharmscitech.org.

30. Subramanian N, Yajnik A, Murthy RSR. Artificial neural networks as an alternative to multiple regression analysis in optimizing formulation parameters of cytarabine liposomes. *AAPS PharmSciTech*. 2004;5(1):Article 4. Available at: http://www.aapspharmscitech.org.

31. Nelson MM, Illingworth WW. *A Practical Guide to Neural Nets*. 4th ed. Reading, MA: Addison-Wesley Publishing Company; 1992.

32. Principe JC, Euliano NR, Lefebvre WC. *Neural and Adaptive Systems: Fundamentals Through Simulations*. New York, NY: John Wiley and Sons; 1999.

33. Wilding IR, Coupe AJ, Davis SS. The role of gamma-scintigraphy in oral drug delivery. *Adv Drug Deliv Rev*. 2001;46(1-3):103-124.

34. Hopfenberg HB. In: Paul DR, Haris FW, eds. Controlled Release Polymeric Formulations (ACS Symposium Series No. 33), American Chemical Society, Washington, DC, 1976. 26–31.